

*Citation for published version:*

Oehlers, DJ, Visintin, P, Chen, JF & Ibell, TJ 2014, 'Simulating reinforced concrete members. Part 2: Displacement-based analyses', *Proceedings of the Institution of Civil Engineers-Structures and Buildings*, vol. 167, no. 12, pp. 718-727. <https://doi.org/10.1680/stbu.13.00072>

*DOI:*

[10.1680/stbu.13.00072](https://doi.org/10.1680/stbu.13.00072)

*Publication date:*

2014

*Document Version*

Peer reviewed version

[Link to publication](https://doi.org/10.1680/stbu.13.00072)

The final publication is available at ICE publishing via <https://doi.org/10.1680/stbu.13.00072>

## University of Bath

### Alternative formats

If you require this document in an alternative format, please contact:  
[openaccess@bath.ac.uk](mailto:openaccess@bath.ac.uk)

#### General rights

Copyright and moral rights for the publications made accessible in the public portal are retained by the authors and/or other copyright owners and it is a condition of accessing publications that users recognise and abide by the legal requirements associated with these rights.

#### Take down policy

If you believe that this document breaches copyright please contact us providing details, and we will remove access to the work immediately and investigate your claim.

# Simulating RC members

## Part 2: displacement based analyses

### **Deric J. Oehlers**

Emeritus Professor, School of Civil, Environmental and Mining Engineering,  
University of Adelaide, Adelaide, Australia

### **Phillip Visintin**

Lecturer, School of Civil, Environmental and Mining Engineering, University of  
Adelaide, Adelaide, Australia

### **Jian-Fei Chen**

Professor, School of Planning, Architecture and Civil Engineering, Queen's  
University Belfast, Belfast, United Kingdom.

### **Tim J. Ibell**

Professor, Department of Architecture and Civil Engineering, University of Bath  
Bath, United Kingdom.

**In a companion paper, the partial-interaction localised properties that require the development of pseudo properties has been described. If the quantification through experimental testing of these pseudo properties could be removed by the use of mechanics based models, which is the subject of this paper, then this would: substantially reduce the cost of developing new RC products by reducing the amount of testing; increase the accuracy of designing existing and novel RC members and structures bearing in mind that experimentally derived pseudo properties are only applicable within the range of the testing from which they were derived; and reduce the cost and increase the accuracy of developing RC design rules. This paper deals with: the development of pseudo properties and behaviours directly through mechanics, as opposed to experimental testing, and their incorporation into member global simulations; and the need for a fundamental shift to displacement based analyses as opposed to strain based analyses.**

*Keywords:* beams & girders; columns; concrete structures; material properties; mathematical modelling; design methods and aids.

### **Notation**

$A_c$	cross-sectional area of concrete
$A_r$	cross-sectional area of reinforcement
$b$	width of section
$c$	concrete cover to centre of reinforcement
$d$	depth of section
$d_{cr-p}$	primary crack height
$d_{NA}$	depth to neutral axis
$d\delta/dx$	slip strain
$E_c$	concrete modulus
$E_r$	reinforcement modulus
$EI$	flexural rigidity

$E_{i-p}$	partial interaction cracked flexural rigidity
$(EI)_u$	uncracked flexural rigidity
$(EI)_c$	cracked flexural rigidity
$F$	force
$f_c$	concrete compressive strength
$f_t$	concrete tensile strength
$jd$	lever arm between the resultant of the flexural tensile and compressive force
$k_e$	bond stiffness = $\tau/\delta$
$L$	length of cylinder or prism
$L_{def}$	half segment length
$M$	moment
$M_a/V_a$	shear span
$N_c$	component of $P_c$ normal to sliding plane
$P$	axial force in reinforcement at a crack; applied load
$P_c$	axial force in concrete element
$S$	shear force along sliding plane
$S_{cr}$	primary crack spacing
$T_c$	component of $P_c$ along sliding plane
$V$	shear force
$V_{sl}$	shear sliding capacity of a section without stirrups
$w$	crack width; widening across sliding plane
$\Delta$	reinforcement slip relative to crack face; half crack width
$\Delta d$	lateral slip
$\Delta L$	longitudinal slip
$\Delta P$	change in $P$ due to shear sliding
$\Delta_{ss}$	slip due to shear sliding
$\Delta_w$	maximum $\Delta L$ of wedge
$\Delta\sigma_n$	change in $\sigma_n$ due to shear sliding
$\alpha$	wedge angle
$\beta_{CDC}$	angle of the critical diagonal crack
$\chi$	curvature
$\delta$	slip along sliding plane
$\delta_{max}$	slip when $\tau$ tends to zero
$\epsilon$	strain
$\epsilon_a$	axial strain
$\epsilon_{asc}$	strain in ascending branch
$\epsilon_{branch}$	total strain in concrete
$\epsilon_{cc}$	material strain in concrete
$\epsilon_{des}$	strain in descending branch
$\epsilon_{mat}$	material strain
$\epsilon_r$	axial strain in reinforcement
$(\epsilon_r)_{eff}$	effective strain allowing for tension stiffening
$\theta$	Euler Bernoulli rotation
$\sigma$	stress
$\sigma_a$	axial stress
$\sigma_n$	stress normal to sliding plane
$\sigma_r$	stress in reinforcement

$\sigma_s$	stress at start of softening
$\tau$	shear stress

## 1. Introduction

Simulating what actually occurs in practice is important because if the local mechanisms that control the global behaviour of RC members are directly simulated through the use of mechanics models there is, in theory, no limit to the use of the model. In contrast, if the local mechanisms are accommodated through the use of pseudo properties that are determined through experimental testing then the model should be limited to within the range of tests from which the pseudo properties were derived which can be very restrictive and produce an unduly conservative design. Furthermore, large scatters exist when the real local mechanism, such as bond-slip, is not included in the model. This scatter can be reduced by extensive testing but there is a limit to the reduction of the scatter when the correct mechanism is not included. To satisfy safety requirements for design, large scatters in the model require large partial safety factors to be used which can make the design very conservative and uneconomical. However, the partial safety factors cannot be too large to be totally uneconomical, which means that some designs are un-conservative, especially for those whose behaviour was not well understood under the given actions.

The challenge of modelling localised deformations also exists in finite element analysis of RC members. There are two common approaches for modelling concrete cracking, that is, the discrete-crack model, and the smeared crack model as a pseudo property. The former simulates a crack as a geometrical identity so discontinuities arising from cracking, that are seen and measured in practice, are physically modelled. In this method, the cracks are commonly defined along element boundaries (Yang et al. 2009), but this inevitably introduces mesh bias. Attempts have been made to solve this problem by developing automatic re-meshing algorithms (Yang and Chen 2005) but overcoming computational difficulties associated with topology changes due to re-meshing is still a challenge in RC members with multiple complex crack patterns.

The smeared crack model treats cracked concrete as a continuum and simulates the deterioration process of cracked concrete using a constitutive relationship and hence smears cracks over the continuum. Hence this is a pseudo property with its consequential limitations and difficulties particularly if determined experimentally. Without due consideration to the strain localisation phenomenon due to cracking, the results are mesh dependent, so that they are not of general value, because the energy consumed during crack propagation approaches zero when the element size approaches zero. Various 'localisation limiters' have been proposed to overcome this mesh non-objectivity problem (Bazant and Planas 1998; Chen et al 2012). However, it needs to be emphasised that the purpose of this paper is not a discussion of finite element methods but rather a discussion of the need for a fundamental shift to displacement based analyses, be it through the implementation of the moment/rotation ( $M/\theta$ ) approached presented in this paper or through finite element analyses, to help accurately simulate the generic RC member behaviour.

Having explained and defined PI material properties and mechanisms in the companion paper (Oehlers et al 2013), to help simplify the incredible complexity of RC member behaviour, we will:

- Outline the displacement based moment-rotation ( $M/\theta$ ) segmental analysis which incorporates the PI mechanisms controlled by the PI material properties
- Show how the displacement based ( $M/\theta$ ) approach is used to analyse not only flexural members but also members that fail in shear.
- Show how difficult it is to quantify pseudo properties through experimental testing.
- Explain how mechanics based solutions can lead to more accurate and widely applicable design procedures and consequently lead to reduced costs.
- Discuss the different forms of modelling and the need for sophisticated models that will reduce the cost of development.

## 2. Euler-Bernoulli moment rotation analysis

The PI mechanisms that occur within an RC member as described in the companion paper (Oehlers et al 2013) are now incorporated into a member analysis for both flexure and shear based directly on the Euler-Bernoulli fundamental theorem of plane sections remaining plane.

### 2.1 Flexure

To determine the effect of the PI mechanisms on the behaviour of a member with the cross-section in Figure 1(b), it is necessary to consider a small segment of the member of length  $2L_{def}$  as in Figure 1(a) (Haskett et al 2009a, 2009b; Oehlers et al 2011; Visintin et al. 2012). The segment is subjected to a constant moment as shown. The straight ends of the segment A-A are rotated by  $\theta$  to the line B-B such that the Euler-Bernoulli theorem of plane sections remaining plane is adhered to. It may be worth emphasising that the direct application of plane sections remaining plane that is the rotation  $\theta$  in Figure 1(a) is a displacement based approach as opposed to a strain based approach. By symmetry, the right hand side of the segment over the length  $L_{def}$  behaves in an identical fashion to that of the left hand side so let us consider the analysis of the left hand side as shown in Figure 2.

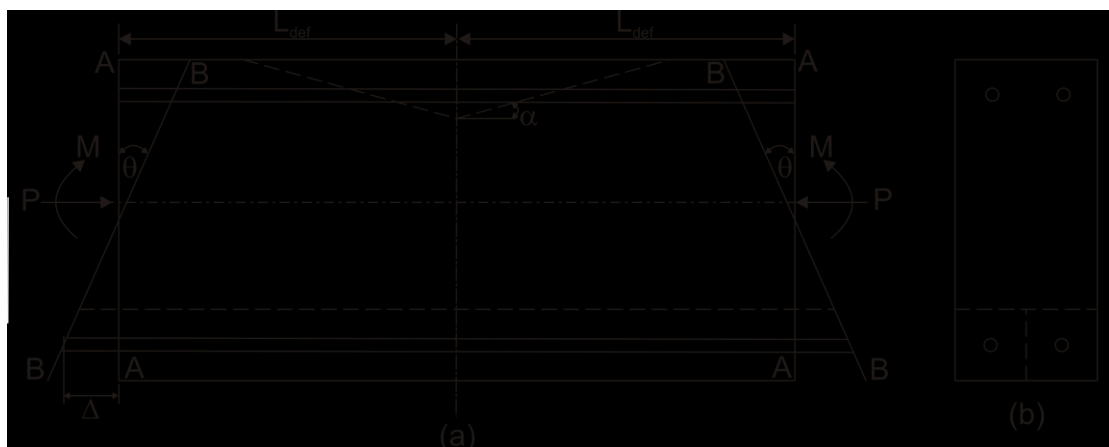


Figure 1. Euler-Bernoulli deformation of segment

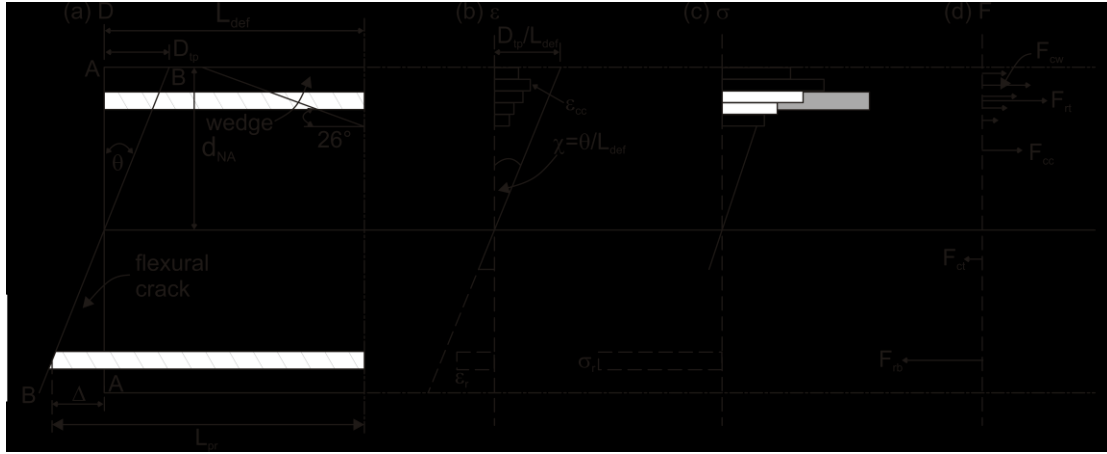


Figure 2. Euler-Bernoulli flexural analysis

In Figure 2(a), the distance between the lines A-A and B-B is the longitudinal deformation within the segment of length  $L_{def}$ . There is a linear variation in deformation based on the above assumption. Dividing this deformation by  $L_{def}$  gives a linear variation in strain as in Figure 2(b) which is the corollary of the Euler-Bernoulli theorem. Prior to concrete softening through the formation of a wedge and prior to flexural cracking, the deformations are strain based so that the stresses in Figure 2(c) can be derived from the material constitutive relationship. From the stress distribution, can be derived the forces in Figure 2(d). For a given applied moment  $M$  and axial load  $P$  it is a question of finding the rotation  $\theta$  and the depth of neutral axis  $d_{NA}$  that achieves equilibrium. This analysis is exactly the same as the generally used moment-curvature ( $M/\chi$ ) analysis which starts with the Euler-Bernoulli corollary of a linear strain profile, that is it starts with the strain profile in Figure 2(b).

In the strain based  $M/\chi$  approach and prior to flexural cracking, the analysis assumes full-interaction that is there is no slip between the reinforcements and concrete so that there is no discontinuity in the strain profile. The  $M/\chi$  approach can allow for cracking as shown in Figure 2(b) but in this case the cracked concrete is totally ignored so that in the tension region the analysis deals with no-interaction that is the interface bond has no strength. Hence the uncracked analysis is a full-interaction analysis, whereas the cracked analysis is both a full interaction and a no interaction analysis which is an anomaly and an approximation in mechanics terms.

To allow for the mechanics of tension-stiffening, the partial interaction analysis in Figure 3, which has already been described in the companion paper by Oehlers et al (2013), can be used to determine the crack spacing  $S_{cr}$  as shown in Figure 3(d). Using this length  $S_{cr}$  as the length of the segment  $2L_{def}$  in Figure 1, the analysis in Figure 4(b), also described in the companion paper (Oehlers et al 2013), gives the relationship between the force in the reinforcement  $P$  and the slip at the crack face  $\Delta$ ; this can then be used in Figure 2(a) to derive the force in the reinforcement  $F_{rb}$  in Figure 2(d) when the half crack width is  $\Delta$ . Hence the strain in the reinforcement  $\epsilon_r$  in Figure 2(b) and the stress in the reinforcement  $\sigma_r$  in Figure 2(c) is no longer dependent on the Euler-Bernoulli corollary of a linear strain profile but on the Euler-Bernoulli theorem of plane sections and in which the analysis allows for the bond slip, that is partial-interaction.

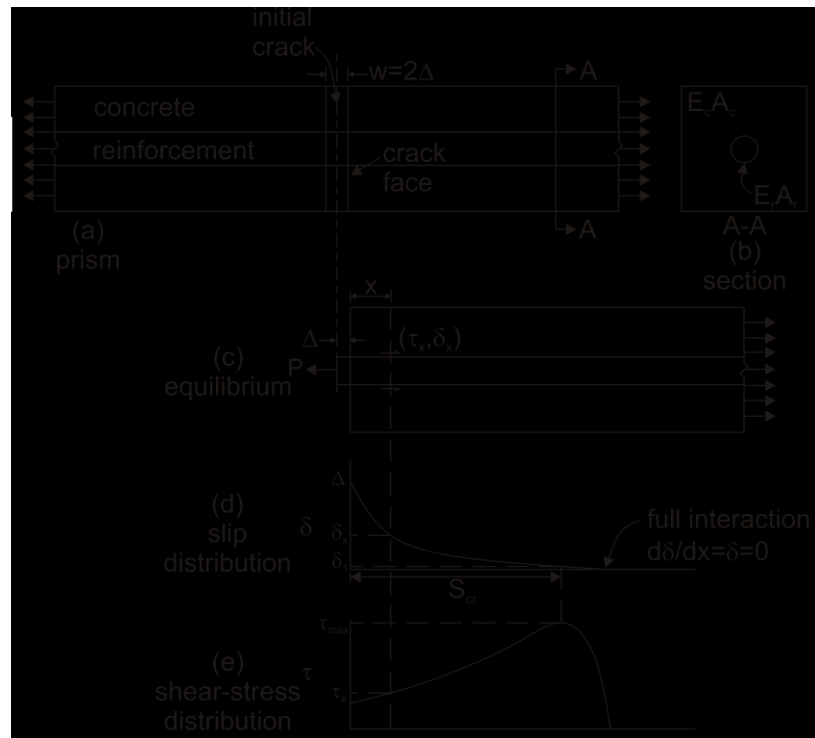


Figure 3. Bond-slip mechanism

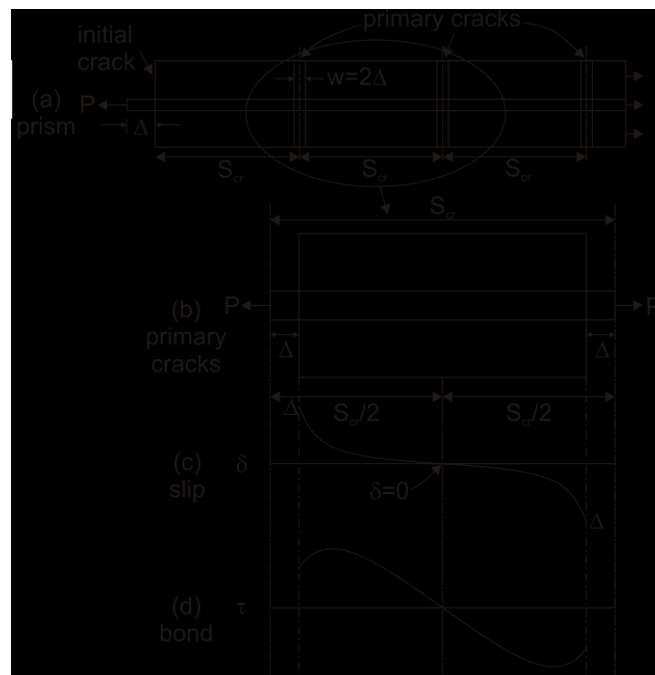


Figure 4. Tension-stiffening mechanism





time dependent effects of creep, shrinkage and relaxation in the analysis in Figure 2 (Visintin et al 2013b).

## 2.2 Flexure/Shear

The analysis in Figure 2 can also be applied to segments subjected to shear and consequently inclined planes as in Figure 7(a) (Shave et al 2007; Lucas et al 2011; Zhang 2013). This segment exhibits the three partial-interaction sliding mechanisms already described (Oehlers et al 2013). The Euler-Bernoulli principal of plane sections remaining plane is applied to the left side of the segment and because the length of the segment varies it produces a non-linear effective strain profile as in Figure 7(b). Hence the corollary of the Euler-Bernoulli theorem that of a linear strain profile is no longer applicable. The analysis in Figure 3 can be used to derive the crack spacing  $S_{cr}$  in Figure 7(a). A diagonal shear crack can emanate from any of these flexural cracks.

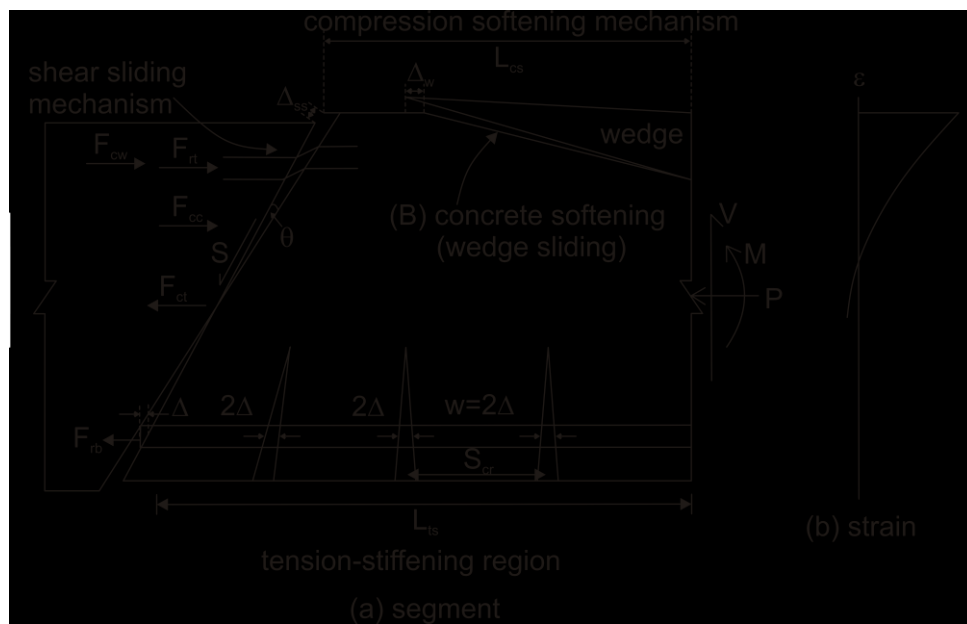


Figure 7. PI mechanisms in RC members subjected to shear

The tension stiffening analysis in Figure 4 can be used for each segment between cracks in Figure 7 to derive the total deformation and consequently the force in the tension reinforcement  $F_{rb}$ ; this depends on, among other things, on the PI bond-slip property (Oehlers et al 2013). The concrete softening analysis in Figure 5 can be used to quantify the compressive stresses in the region where a wedge forms in Figure 7(a) using the PI shear-friction properties (Oehlers et al 2013). And finally, the PI shear-sliding mechanism in Figure 8, already described in the companion paper (Oehlers et al 2013), in conjunction with the flexural forces across the sliding plane in Figure 7(a) can be used to quantify the shear capacity. Importantly, it can be seen that the shear capacity depends on the flexural forces that confine the sliding plane and, hence, shear behaviour depends directly on the flexural forces.

## 3. Variation in pseudo material properties

It has been shown above how the PI mechanisms that are induced by the PI material properties can be incorporated into a member behaviour through the use of a

displacement based segmental approach, that is through the direct use of the Euler-Bernoulli theorem of plane sections remaining plane. An alternative approach, and commonly used, is to start with the corollary of the Euler-Bernoulli theorem that of a linear strain profile, that is a strain based approach as illustrated in Figure 2(b). In this case, all the behaviours associated with the PI mechanisms due to the PI material properties, as described in the previous section, have to be represented in a strain based form, that is, as a pseudo material property. Unlike material properties which are fixed for a specific material, pseudo properties not only depend on the material properties but also on the geometry, and restraints and loading applied to the member and, hence, vary widely as will be illustrated.

### 3.1 Pseudo $\sigma/\epsilon$ tension stiffening

The tension stiffening mechanism has already been illustrated in Figures 4(b). In its simplest form, it is the relationship between the stress in the reinforcement at a crack face  $\sigma_r$ , that is  $P/A_r$ , and the effective strain  $(\epsilon_r)_{\text{eff}}$ , that is  $2\Delta/S_{\text{cr}}$  which is the effective (average) strain in the partial-interaction region due to both the concrete cracking and the concrete encasing the reinforcement which leads to a non-uniform strain distribution in the reinforcement. These pseudo material properties  $(\sigma_r/(\epsilon_r)_{\text{eff}})$  can be used in the moment-curvature  $(M/\chi)$  strain based approach in Figure 2(b). Hence it is a question of quantifying the effective strain  $(\epsilon_r)_{\text{eff}}$  for use in a strain based approach.

It can be seen from Figures 3 and 4 that the tension stiffening behaviour and consequently the effective strain due to tension stiffening  $(\epsilon_r)_{\text{eff}}$  depends on: the moduli of the concrete  $E_c$  and reinforcement  $E_r$  in Figure 3(b); the bond-slip property  $\tau/\delta$  (Oehlers et al 2013); the cross-sectional area of the reinforcement  $A_r$  and concrete  $A_c$  in Figure 3(b); the crack spacing which depends on whether there are primary cracks of spacing  $S_{\text{cr}}$  in Figures 3 and 4 or secondary cracks of spacing  $S_{\text{cr}}/2$ ; the boundary conditions such as  $d\delta/dx = \delta = 0$  in Figure 8(c) and  $\delta=0$  in Figure 4(c); and, of course, on the stress in the reinforcement at the cracked section  $P/A_r$  in Figures 3 and 4. This complexity or difficulty is further illustrated from closed form solutions.

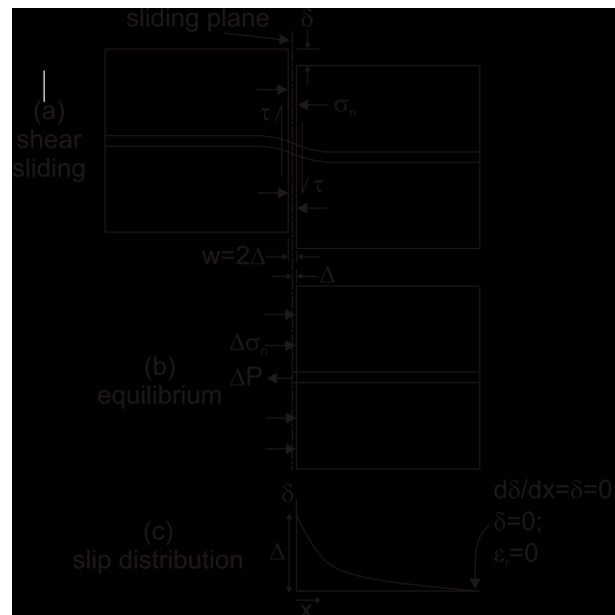


Figure 8. Shear-sliding mechanism

Take for example the simplest of bond-slip properties that of the idealised linear descending bond-slip (Oehlers et al 2013). For this simplest of bond-slip properties and only when primary cracks are present, the effective strain is given by

$$(\varepsilon_r)_{eff} = \frac{\delta_{max} \left(1 - \frac{1}{\cos(\lambda S_{cr}/2)}\right) - \frac{\sigma_r \tan(\lambda S_{cr}/2)}{E_r \lambda}}{S_{cr}/2} \quad (1)$$

in which the primary crack spacing is given by

$$S_{cr} = \frac{\arcsin\left(\frac{\sigma_r}{E_r \lambda \delta_{max}}\right)}{\lambda} \quad (2)$$

and where  $\lambda$  is a function of both the bond-slip properties and geometric properties (Muhammed et al 2012; Muhammed et al 2013). It can be seen that the pseudo strain  $(\varepsilon_r)_{eff}$  due to tension stiffening depends not only on the material properties but also on geometries and boundary conditions; this makes it very difficult to extract a pseudo tension stiffening strain for a strain based approach such as in Figure 2(b) from experimental testing.

### 3.2 Pseudo $\sigma/\varepsilon$ concrete compressive softening

An element in a compression test as in Figure 9, as explained in the companion paper (Oehlers et al 2013), contracts due to material contraction and due to sliding as shown in Figure 9 and further illustrated in Figure 5. The sliding component  $\Delta L$  in Figure 5 can be determined from the shear friction material properties (Oehlers et al 2013) which depend not only on the concrete compressive strength but also on the aggregate interlock properties such as aggregate size, shape and strength, and the mortar properties relative to the aggregate properties which, for example, determines whether the sliding plane goes around the aggregate or through the aggregate.

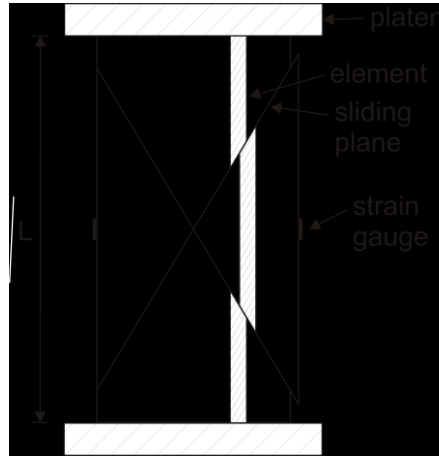


Figure 9. Concrete compression test

A cylinder of concrete fails through the formation of a single set of sliding planes as illustrated in Figure 9. If the height of the cylinder  $L$  is increased, a single set of sliding planes still exists. Consequently, the component due to sliding  $\Delta L$  in Figure 5 remains the same and the only increase in contraction is due to material contraction over the increased length. With this in mind, it can be shown (Chen et al. 2013) that the effective

or pseudo strain can be extracted for a specimen of length  $L_2$  from a test cylinder of length  $L_1$  using the following expression and without the need for the direct use of shear friction properties.

$$((\varepsilon_n)_{branch})_{L_2} = [((\varepsilon_n)_{branch})_{L_1} - (\varepsilon_n)_{mat}] \frac{L_1}{L_2} + (\varepsilon_n)_{mat} \quad (3)$$

where  $n$  is the stress level and the subscript ‘branch’ refers to the ascending or descending branches in Figure 10 (Oehlers et al 2013). For example, if the pseudo stress-strain relationship O-A-C-D was obtained from a cylinder of length  $L_1$ , then from Eq. 3, a cylinder with a greater length  $L_2$  would have the pseudo stress strain relationship shown in Figure 10 which in turn could be used in the displacement based analysis in Figure 1 where  $2L_{def}$  is  $L_2$ .

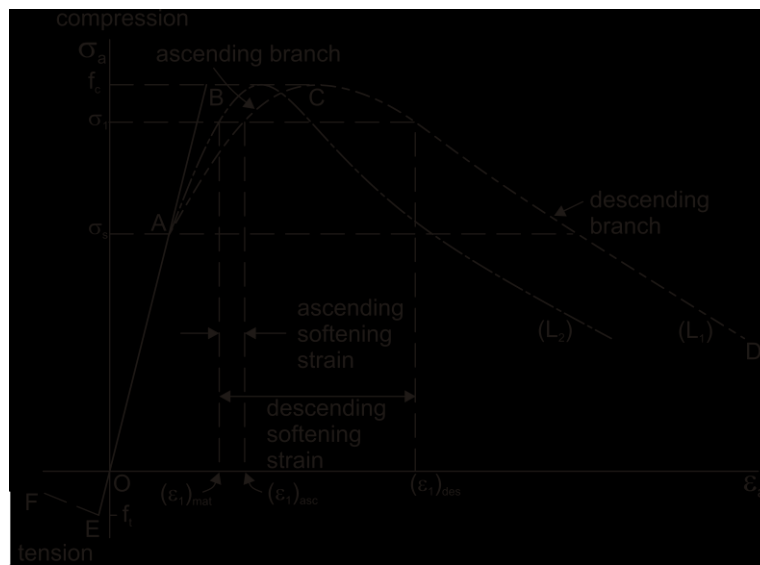


Figure 10. Concrete deformation in strains

Equation 3 clearly shows that that pseudo compressive stress strain relationship is size dependent that is depends on  $L_1/L_2$ . Hence it can only be applied in a strain based  $M/\chi$  approach as in Figure 2(b) for a specific size of segment as in Figure 1 which is often referred to as a hinge. It can be seen that the pseudo compressive stress-strain relationship depends not only on the compressive strength but also on the shear-friction properties and also is size dependent which makes the commonly used research approach of finding a size independent stress-strain relationship difficult to achieve.

### 3.3 Pseudo shear sliding

The shear sliding mechanism in Figure 8 controls the shear behaviour and capacity of RC members and, consequently, experimental tests (Oehlers et al 2013) are frequently conducted to quantify this property. This pseudo shear sliding property depends on all the variables associated with tension stiffening and with compression softening as described above. In addition, the pseudo shear sliding material property depends on the additional variable of the boundary condition of the reinforcement as in Figure 8(c) where: if the reinforcement is long, is the full-interaction boundary condition

$d\delta/dx=\delta=0$ ; for anchored bars is  $\delta=0$ ; and for short bars is  $\varepsilon_r=0$ . Hence quantifying the shear sliding pseudo properties experimentally is not an easy task. Simulating the physical behaviour of RC members subjected to shear as in Figure 7 allows closed form solutions to be derived for the shear capacity (Zhang 2013).

#### 4. Closed form models

Running a numerical model is considerably less expensive than experimental testing so that numerical models that simulate the local physical behaviours can be used in wide ranging parametric studies to develop design rules. A more advanced approach is to develop closed form solutions from the model which not only gives a deep understanding of the mechanism and the parameters that affect the mechanism but also can be used to form the fundamental foundation for the design model.

##### 4.1 Closed form flexural rigidities

Closed form solutions for the flexural rigidity at serviceability can be derived from the segmental analysis in Figures 1 and 2 (Visintin et al 2013a). For the specific case of a segment with only primary cracks and in which the bond-slip stiffness  $k_e = \tau/\delta$  is constant, the sectional effective or pseudo flexural rigidity is given by

$$EI_{pi-p} = \frac{E_c b \tanh(1) (-d^3 + 3d^2 d_{cr-p} - 3d d_{cr-p}^2 + d_{cr-p}^3) + 6A_r E_r (d d_{cr-p} - d_{cr-p} c - d c + c^2)}{6 \tanh(1)} \quad (4)$$

where  $E_c$  and  $E_r$  are the concrete and reinforcement moduli,  $A_r$  is the area of the reinforcement with cover  $c$ ,  $d$  is the depth,  $b$  is the width and  $d_{cr-p}$  is the primary crack height given by

$$d_{cr-p} = \frac{db E_c \tanh(1) + A_r E_r \pm \sqrt{2db E_c A_r E_r \tanh(1) + A_r^2 E_r^2 - 2b E_c A_r E_r c \tanh(1)}}{b E_c \tanh(1)} \quad (5)$$

Empirical research can be divided into that required to define the model and that required to quantify the parameters within the model. Hence the closed form solution of Eqs. 4 and 5 eliminate the need to define the model through experimental tests so that the empirical researcher can now concentrate on quantifying the parameters within the model. For example, researchers could focus their research on finding simple models for  $d_{cr-p}$  in Eq. 5 by using Eq. 5 to perform parametric studies. It is interesting to note that the effective stiffness of Eq. 4 does not depend on the bond-slip stiffness  $k_e$  even though this was included in the derivation. This sounds incorrect but the model shows that the increase in flexural rigidity associated with increasing the bond stiffness is offset by the formation of more cracks. Hence empirical researchers need not bother with varying the bond properties in their tests. This is an example of how closed form solutions can simplify the problem but it also emphasise the difficulty of finding pseudo flexural rigidities from experimental testing.

##### 4.2 Closed form shear capacity

The analysis illustrated in Figure 7 can be used to derive the following closed form solution for the shear capacity at a section without stirrups (Zhang et al 2013)

$$V_{sl} = \frac{bd_{NA}A}{1-C\left(\frac{M_a/V_a - \frac{S_{cr}}{2} \frac{d}{\tan(\beta_{CDC})}}{jd}\right)} \quad (6)$$

where  $b$  is the width of the section,  $d$  the effective depth,  $jd$  the lever arm between the resultant of the flexural tensile and compressive force,  $d_{NA}$  the depth of the compression zone,  $S_{cr}$  the flexural crack spacing, the ratio between the moment and the shear force at the section is  $M_a/V_a$ ,  $\beta_{CDC}$  the angle of the critical diagonal crack, and the coefficients  $A$  and  $C$  quantify the material shear stress capacity. Hence the model has been quantified through mechanics so that the empirical researchers can concentrate their efforts in quantifying the parameters such as  $\beta_{CDC}$ ,  $jd$  and  $d_{NA}$ . It is interesting to note that the shear capacity in Eq. 6 depends to a large extent on the shear span  $M_a/V_a$  and it is this sort of dependency which is difficult to identify empirically.

## 5. Modelling

Listed below are three major tasks in the development of an RC member. This includes: (A) the quantification of the material properties through experimental testing; (B) the quantification of the member behaviour at all limit states which can be done through experimental testing or modelling or a combination of both; and (C) the development of simple design rules from the quantified behaviours which usually includes the testing of large scale members for safety considerations.

- Task A) Quantification of the material properties
- Task B) Quantification of the RC member behaviours
- Task C) Development of Design Rules

A model that simulates through mechanics alone the physical behaviour that the RC member exhibits can be used in conjunction with material properties that are determined experimentally to predict the member behaviour, that is, it can be used for Task (B). The results from Task B can then be used to develop design rules, that is, Task (C). Let us refer to this type of model as a sophisticated model that can directly simulate the physical behaviours of RC members through mechanics; and in which the magnitudes of the physical behaviours depend on the material and geometric properties input into the model. Hence no component of the mechanics of a sophisticated model depends on experimental testing. Hence a model that simulates purely through mechanics the physical behaviour will save testing for Task (B) and development will only require a relatively small amount of material testing for Task (A) and some validation testing at large scale for Task (C).

Current procedures are often a mishmash of approaches. A commonly used approach is to use strain based numerical modelling to quantify the behaviour that is Task B. However the strain based approach itself requires pseudo material properties which are frequently determined from experimental testing which means that most of the testing in Task (B) is in the derivation of the pseudo material properties. In addition, as these pseudo material properties have been derived by tests they can only be used within the bounds of the testing regime from which they were developed. Hence if the strain based model is needed to predict the behaviour of members that have different material properties, have different geometric properties for example they are larger, or have

different loading configurations, then further testing is required for Task (B). Furthermore, it has been shown that trying to quantify pseudo material properties purely through testing is very difficult which invariably leads to very uneconomical approaches in the development of design rules which is detrimental to development.

Another way of viewing the problem is that the emphasis in current modelling is to use a strain based model and then refine the material properties and pseudo material properties to achieve a close fit with the global behaviour of the member such as the load-displacement. There is generally no requirement to ensure that the model simulates the local physical behaviour that can be seen or measured in practice such as the crack spacings or widths or concentrations in rotation. Hence the emphasis is on simulating the global behaviour at the expense of the local behaviour. It is suggested that this approach leads to a large amount of testing and consequently increased cost with little gain. An alternative approach would be to place the emphasis in modelling on simulating, through mechanics, the physical local behaviour that can be seen or measured in practice as this would lead to a large reduction in the cost of development.

## **6. Conclusions**

A large amount of testing in the development of RC products and their associated design rules is to provide pseudo properties for the use of strain based analysis techniques. It has been shown that this approach is very expensive and restrictive. An alternative approach is to use a displacement based approach such as the M/θ approach as this can eliminate the need, through mechanics, of pseudo material properties and, hence, reduce the cost of development of products and design rules. It is suggested that this approach, in which the emphasis is on simulating through mechanics the local physical behaviour of RC members that can be seen or measured in practice, will reduce the amount of testing to develop new products or design rules and, furthermore, allow structural engineers to design members outside the range of experimental tests.

## **Acknowledgements**

The financial support of the Australian research Council ARC Discovery project DP0985828 ‘A unified reinforced concrete model for flexure and shear’ is gratefully acknowledged.

## **References**

- Bazant, Z.P. and Planas, J. (1998). *Fracture and Size Effect in Concrete and Other Quasibrittle Materials*, CRC Press.
- Chen Y, Visintin P, Oehlers DJ and Johnson AU (2013) Size dependent stress-strain model for unconfined concrete Accepted *ASCE Structures* 12/4/13
- Chen, G.M., Chen, J.F. and Teng, J.G. (2012), “On the finite element modelling of RC beams shear-strengthened with FRP”, *Construction and Building Materials*, Vol. 32, No. 7, pp13-26.
- Chen, G.M., Teng, J.G. and Chen, J.F. (2011), “Finite element modeling of intermediate crack debonding in FRP-plated RC beams”, *Journal of Composites for Construction*, ASCE, Vol. 15, No. 3, pp339-353.

- Haskett M, Oehlers DJ, Mohamed Ali MS and Wu C (2009a) Rigid body moment-rotation mechanism for reinforced concrete beam hinges. *Engineering Structures***31**:1032-1041.
- Haskett M, Oehlers DJ, Mohamed Ali and Wu C. (2009b) Yield penetration hinge rotation in reinforced concrete beams. *ASCE Structural Journal*, **135(2)**:130-138.
- Haskett M, Oehlers DJ, and Mohamed Ali MS (2010a) Design for moment redistribution in RC beams retrofitted with steel plates. *Advances in Structural Engineering* **13(2)**:379-391
- Haskett M, Oehlers DJ, Mohamed Ali MS and Wu C (2010b) Analysis of moment redistribution in FRP plated RC beams. *ASCE Composites in Construction* **14(4)**:424-433.
- Lucas W, Oehlers DJ and Mohamed Ali MS (2011) Formulation of a shear resistance mechanism for inclined cracks in RC beams. *ASCE Journal of Structural Engineering***137(12)**:1480-1488.
- Muhamad R, Mohamed Ali MS, Oehlers DJ, and Griffith MC (2012)The tension stiffening mechanism in reinforced concrete prisms. *International Journal of Advances in Structural Engineering***15(12)**:2053-2069.
- Muhamad R, Oehlers DJ, and Mohamed Ali MS (2013) Discrete rotation deflection of reinforced concrete beams at serviceability. *Proc. ICE Structures and Buildings* **166(3)**:111-124.
- Oehlers DJ, Mohamed Ali MS, Haskett M, Lucas, W, Muhamad R, and Visintin P, (2011a) FRP reinforced concrete beams – a unified approach based on IC theory. *ASCE Composites for Construction* **15( 3)**:293-303.
- Oehlers DJ, Visintin P, Chen JF and Ibell TJ (2013) Simulating RC members. Part 1: partial interaction properties. *Submitted Proc. ICE Structures and Buildings*.
- Shave J.D., Ibell, T.J. and Denton S.R. (2007) Shear assessment of reinforced concrete bridges with short anchorage lengths. *The Structural Engineer*, March 6: 30-37.
- Visintin P, Oehlers DJ, Wu C, and Haskett M (2012) A mechanics solution for hinges in RC beams with multiple cracks. *Engineering Structures* **36**:61-69.
- Visintin P, Oehlers DJ, and Haskett M (2013b) Partial-interaction time dependent behaviour of reinforced concrete beams *Engineering Structures***49**: 408-420.
- Visintin P, Oehlers DJ, Muhamad R and Wu C (2013a) Partial-interaction short term serviceability deflection of FRP RC beams. Accepted *Engineering Structures* 14/6/13.
- Visintin P, Oehlers DJ, Muhamad R and Wu C (2013a) Partial-interaction short term serviceability deflection of FRP RC beams. Accepted *Engineering Structures* 14/6/13.



- Yang, Z.J. and Chen, J.F. (2005), "Finite element modelling of multiple cohesive discrete crack propagation in reinforced concrete beams", *Engineering Fracture Mechanics*, Vol. 72, No. 14, pp2280-2297.
- Yang, Z.J., Su, X.T., Chen, J.F. and Liu, G.H. (2009), "Monte Carlo simulation of complex cohesive fracture in random heterogeneous quasi-brittle materials", *International Journal of Solids and Structures*, Vol. 46, No. 17, pp 3222-3234.
- Zhang, T (2013) A mechanics based approach for shear strength of RC beams without web reinforcement. *Departmental report*, No. R 184, the University of Adelaide, Australia.
- Zhang, T., Visintin, P., Oehlers, D.J (2013) Shear strength of RC beams without stirrups. Submitted for publication in *ICE Structures and Buildings*.